Phase transitions in a resonating free-piston engine generator

Julian Dunne

Phase Transitions in a Resonating Free-Piston Engine Generator

Julian F. DUNNE

Univ of Sussex, Falmer, Brighton, UK. BN19QT
j.f.dunne@sussex.ac.uk

Abstract

The phase difference between the excitation force and the response of a resonating free piston engine generator, has been examined by numerical simulation, for both resonant starting, and self-excited resonant operation. This is achieved by using a simple nonlinear model of a resonating free piston generator, first undergoing resonant starting, then undergoing a self-excited resonant Otto cycle. The resonant starting results show that the system is highly sensitive to very small changes in both amplitude and frequency. The resonant starting results also show that with harmonic excitation at the operational resonant frequency, the response phase is only moderately delayed behind the excitation.

Under resonant operating conditions, the phase difference between the fundamental harmonic component of the self-excitation, and the fundamental harmonic component of the displacement response have also been obtained by simulation, and found to be very small, suggesting the excitation and response are almost in phase. The implications of this finding in making the transition from resonant starting to self-excited operation (involving fired combustion) are assessed and appropriate guidance given.

1 Introduction

Free-piston engine generators (FPEGs) offer a number of important benefits over conventional generators, the latter comprising an engine coupled directly to an electrical generator [1][2]. The benefits of FPEGs include higher efficiencies, greater compactness, and lighter weight, resulting in significantly higher gravimetric and volumetric energy densities, compared to alternatives. In addition, the unlimited scalability to high power of an FPEG, and the possibility of electrically-controlled variable compression ratio, offers fuel flexibility and the potential to run on zero carbon fuels [3 - 11].

Resonating FPEGs [12][13] offer significant advantages over FPEGs that use a bounce chamber. These advantages include more precise control, a significant reduction in electrical machine currents, and a corresponding reduction in electrical power losses. The fitting of a stiff resilient member within an FPEG, creates a mass-elastic system capable of mechanical resonance. Resonating rotary FPEGs [12] offer additional advantages over resonating linear FPEGs, in particular, no loss of symmetry. In terms of dynamic characterisation in operation, a resonating FPEG is actually a nonlinear (stochastic) self-excited system. The main source of nonlinearity stems from the polytropic gas compression and expansion processes that take place as the free pistons move in the cylinder. The categorisation of the system as ‘self-excited’ stems from the combustion ‘timing’ which largely depends on the particular displacement of the pistons.

The use of mechanical resonance can also be important for starting a resonating FPEG. In particular, resonance is an essential way of getting a resonating FPEG up to the required displacement amplitude needed for combustion to occur since the resilient members tend to be very stiff. Starting can in principle be achieved by motoring the electrical machine with a relatively low-power external excitation source, such as a harmonic or optimal exciter signal [14]. This is an analogous procedure to the use of square wave external excitation source for starting an FPEG fitted with a bounce chamber [15] - although in the latter case, resonance is not necessarily exploited.

A significant difficulty using mechanical resonance to start a resonating FPEG, is first to recognise a fundamental difference between starting and steady operation. In resonant starting, the fundamental harmonic component of the steady-state response (of any lightly damped linear system), is very close to $\pi/2$ radians out-of-phase from the external harmonic excitation. But in operation, under self-excited resonant conditions, the phase difference between the dynamic response and the excitation, can be significantly different from $\pi/2$. This reality leads to three questions.

First, in resonant starting, how does system nonlinearity (from adiabatic compression and expansion processes) affect the phase difference between the excitation and response? (which, for a linear system, is close to $\pi/2$). Second, in operation, what is the phase difference be between the self-excitation process (resulting from combustion) and the corresponding dynamic response? The third question is how is it possible to be guided in making the transition from externally-excited resonance (used for starting) to self-exited steady-state resonant operation? In this paper, these three questions are examined by modelling and simulation. The objective is to provide clear guidance on how to transition between resonant starting and subsequent self-excited operation of a resonating free-piston engine generator.

2 A dynamic model for resonating free-piston generator operation

Here, a linear resonating free piston generator is modelled by first considering the physical model displacement variables. Then, an equation of motion is constructed to include a description of the processes involved.

2.1 The physical model displacement variables and the equation of motion

Figure 1a shows a simple diagram of a resonating linear FPEG comprising: opposed pistons, generators and rods, and very stiff springs. The various displacement variables associated with the generator simulation model are shown in Figure 1b. A single side of an opposed-piston FPEG is shown in Figure 1a by assuming symmetric operation of an opposed-piston generator.

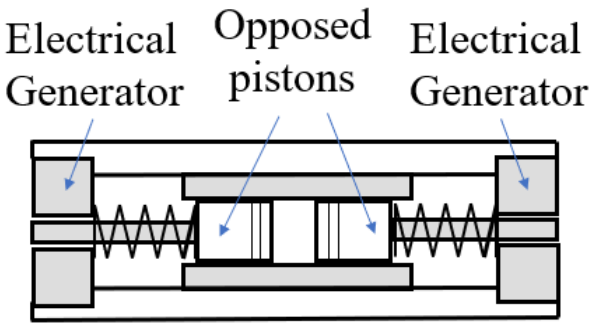

Figure 1a: Resonating linear free piston generator

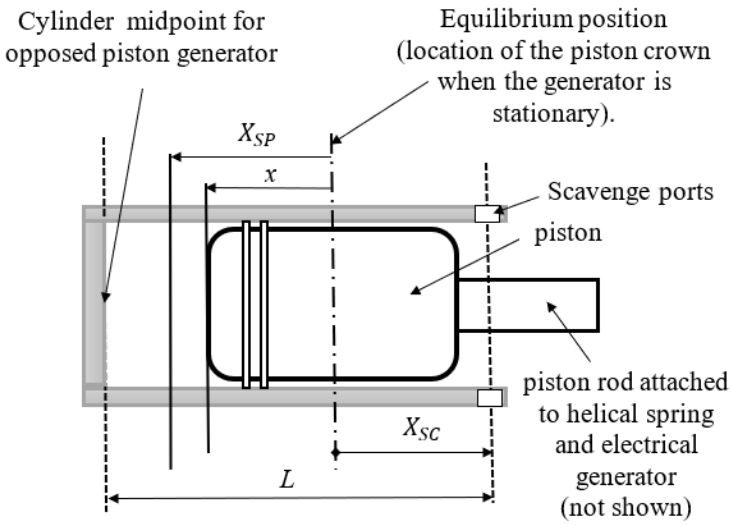

Figure 1b: Free-piston generator position variables.

Focusing on a two-stroke Otto cycle, in particular, where key events occur spatially, four different parts of an Otto cycle can be identified. The variable x in Figure 1b is the instantaneous position of piston (crown) relative to the equilibrium position. The equilibrium position is the location of the piston crown when the generator is stationary. X_{SP} is the sparking position (i.e. the distance relative to equilibrium position) where instantaneous combustion is assumed to occur causing a rise in cylinder pressure. Position X_{SC} (which has a negative length value) is the distance from the equilibrium position to the scavenge ports. Distance *L* is the length along the cylinder from the scavenge ports to the midpoint of the cylinder in an opposed piston engine. Since L+X_{SC} gives the distance from the equilibrium position to the midpoint of the cylinder, in a simulation if $x \geq$ L+X_{SC}, then the very undesirable event of contact between the opposed pistons would have been made. Application of Newton's 2nd law to the piston and electrical machine, gives an equation of motion:

$$m\ddot{x} + c_g\dot{x} + f(x,\dot{x}) + kx = e(t) - AP(x(t)) \quad (1)$$

where m is the total mass of the moving assembly (i.e. the piston, rod, and the moving electrical machine), A is the piston area, $P(x)$ is the cylinder pressure (which is a nonlinear function of the piston displacement), c_g is an electrical machine constant, *k* is the helical spring stiffness, $e(t)$ is the motoring (excitation) force, and $f(x,\dot{x})$ is a friction force. Here for simplicity, it is assumed that the scavenging model is one where exhausting occurs at the same instant as the scavenging ports are uncovered i.e. when the piston position is at -X_{SC}. This is more appropriate for uniflow scavenge than loop scavenge. The electrical generator load model is assumed to be proportional to the electrical machine velocity, such that the opposing force while generating, is $c_g\dot{x}$. The instantaneous generated power (assuming 100% efficient generation) is then $c_g\dot{x}^2$.

The cylinder pressure $P(x)$ is assumed to follow adiabatic compression from scavenge port closure until to the sparking position. Instantaneous combustion heat release is assumed to occur when the sparking position is reached, leading to a rise in cylinder pressure dP_{max} producing maximum pressure of Pmax. Pressure above the sparking position is assumed to remain at Pmax, although, by suitable choice of sparking position, it is possible to arrange in a simulation, for the maximum piston motion to never exceed the sparking position. Adiabatic expansion is assumed from Pmax to P_0, i.e. to the point where the scavenge ports are uncovered. No distinction is made between the exhaust port level, and scavenge port level. Exhausting is therefore assumed to take place at the same time as scavenging. The cylinder pressure model from x=Xsc to x=Xsp is:

$$P(x(t)) = (\mathrm{Vin}/\mathrm{V})^{\gamma} \times \mathrm{Pscav} \quad (2)$$

where γ is the adiabatic index, Pscav is the scavenge pressure, $\mathrm{Vin} = \mathrm{LA}$ is the effective initial volume, and $\mathrm{V} = (\mathrm{L} - (x(t) - Xsc))\mathrm{A}$ is the instantaneous volume. During expansion, from x=Xsp to x=Xsc, with Pmax as the peak pressure after heat release, the cylinder pressure is given by:

$$P(x(t)) = (\mathrm{Vin}/\mathrm{V})^{\gamma} \times \mathrm{Pmax} \quad (3)$$

3 A bi-linear model for conditionally-stable cyclic motion without control

In general, a free piston engine does not have a mechanical cycle because the piston does not necessarily return to the same position. In fact, feedback control is generally needed in a resonating FPEG to ensure that the cycle returns to the same starting position [12]. Without feedback control the cycle will be unstable – either the generator will stall, or the piston amplitude will continue to grow until collision takes place between the piston crowns. A typical control strategy involves multi-variables, to achieve control of fuel (i.e. energy in), and spark timing to control the start of heat release, and control of the electrical generator load (i.e. output energy). But because the objective is to understand the phase differences between excitation and response, feedback control will not be used to create a stable cycle. Rather, a passive change in the generator load parameter is achieved for part of the cycle – this enables a conditionally-stable cycle to be achieved. More will be said about this in Section 5.

4 Nonlinear phase-shifting during resonant starting

The first phase-shifting question of interest, is what happens to the phase difference between the excitation, needed for (resonant) starting, and the dynamic response as a result of adiabatic compression and expansion which, although of much weaker stiffness than the resilient springs, introduce significant nonlinearity. Various strategies are available to start a free piston engine [14]. Here only the simplest strategy will be considered, namely exciting it with a single harmonic at its resonant frequency. Were the system to remain entirely linear, for any periodic external excitation, theory suggests that the fundamental harmonic component of the steady-state response (for a lightly damped linear system), would be very close to π/2 radians out-of-phase from the fundamental harmonic component of the excitation (the phase difference between the excitation and the response, at the natural frequency, is exactly π/2 radians regardless of the damping level (and if the damping is light, the natural frequency and the resonant frequency are very close). To answer this question, the phase difference between the fundamental components of the excitation and response is obtained by numerically using model Equation (1) driven externally by sinusoidal excitation involving adiabatic compression and expansion but without ignition occurring.

Here, a generator of moving mass m=0.42 kg is assumed in Equation (1), and the resilient spring stiffness k = 60000 N/m. A single fixed value for the electrical machine coefficient power take-off is assumed of magnitude c_g=5.20, which effectively appears as a 'damping' coefficient in Equation (1). For these parameters, ignoring the nonlinear adiabatic effects, the 'damping' factor is 1.63% critical, i.e. very light damping. The small friction force $f(x,\dot{x})$ is ignored. A sinusoidal excitation force $e(t)$ at the nonlinear resonant frequency, was chosen of fixed amplitude 215 N. In computing the phase difference, the Matlab initial value function *ode45* was used to solve for 100 transient cycles. A complete period of the last cycle of the nonlinear response was used to establish the phase difference between the excitation and the phase by using the Matlab Fourier analysis function *fft* to obtain the Fourier coefficients. Were the system entirely linear, and if it were excited at the linear resonant frequency of 59.98 Hz, the theoretical phase difference would be -89.0638° (i.e. a delay very close to π/2 radians out-of-phase). However, exciting at the actually (nonlinear) resonant frequency of 78.994 Hz, the phase difference between the response fundamental harmonic and the excitation = -15.25°. Figure 2 shows the simulated excitation (top) and (nonlinear) resonant response (bottom).

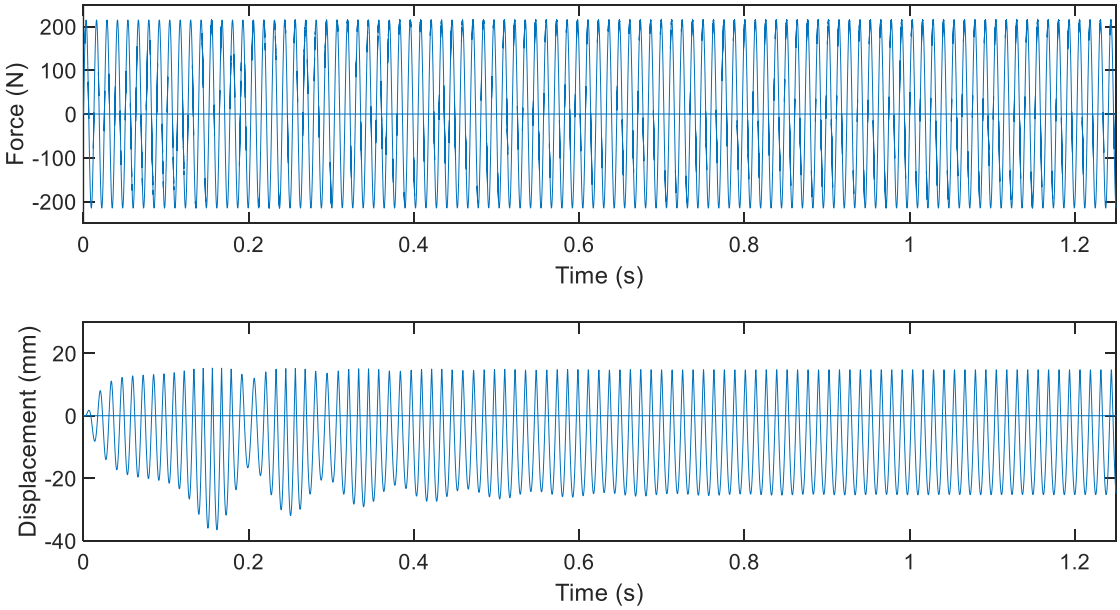

Figure 2: Harmonic excitation (top) and response (bottom) showing steady-state being reached.

To illustrate the computed nonlinear phase difference, which is a massively reduced delay, Figure 3 (top) shows a section of the last cycle of the excitation (which actually includes two plots, namely, the chosen sinusoidal excitation function, plus an additional plot of the excitation function obtained from *within* the ode45 function, to ensure complete synchronicity - confirmed by no evidence of any difference). Figure 3 (bottom) shows the corresponding section of the fundamental harmonic of the displacement response.

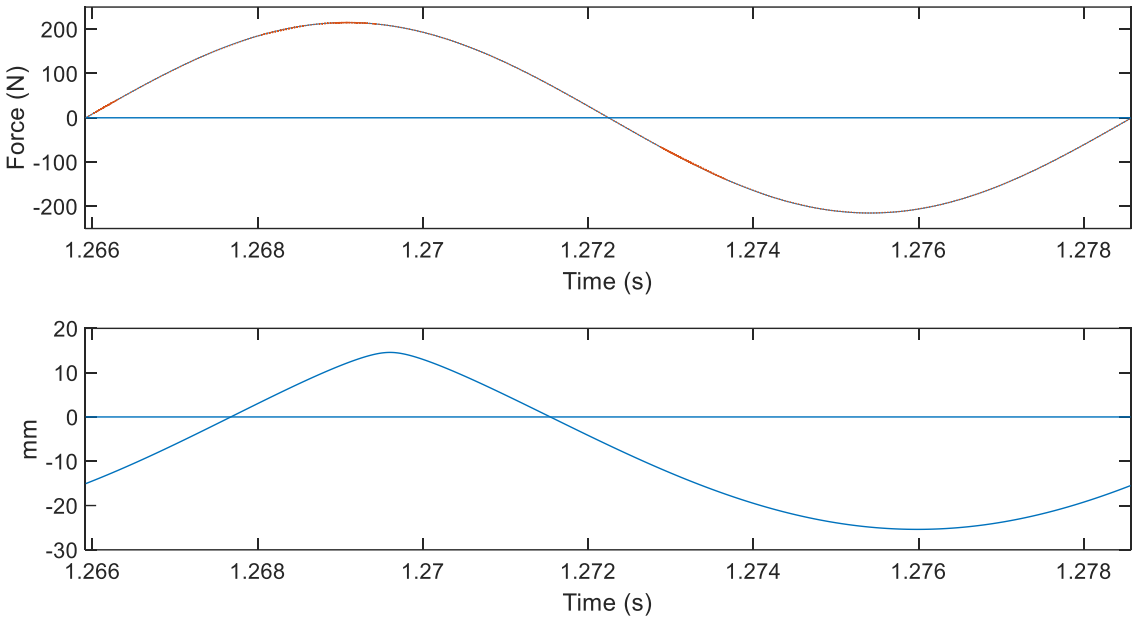

Figure 3: The excitation (top) and the steady-state displacement response (bottom)

5 The phase difference between self-excitation and the resonant response.

The next question concerns the phase difference between the self-excitation process (resulting from timed-combustion) and the corresponding dynamic response. Here, the assumption is that the generator has been successfully started, and that a continuous series of stable cycles is achievable. In actual fact, as mentioned previously, stable operation of a resonating FPEG is generally only possible with feedback control of both the combustion heat release and the electrical generator [12]. This applies even without the influence of cycle-by-cycle stochastic variability in the combustion pressure. Thus, even without cycle-by-cycle variability, this effectively means that the combustion gas pressure P(x(t)), and the generator coefficient c_g in Equation (1), need to be actively controlled to ensure that a target piston displacement is maintained. In actual fact, what ideally needs to be found, is the phase difference between the combustion excitation and a stable displacement response *without* active control being involved, because control itself will significantly change the phase difference.

To address this question, a way has to be found to create a conditionally-stable (repetitive) cycle without feedback control. To do this, the solution is to choose switched values of the generator coefficient c_g to ensure that the generator state vector returns precisely to the same starting point. This does not actually guarantee stability *in the large* (which is why it is referred to as conditional stability). Two values of c_g are however sufficient to achieve conditional stability – a constant value during compression, and a different (larger value) during expansion (the power stroke). In practice, different values of c_g can only be implemented, at the frequency needed, using power electronic switching.

5.1 Numerical simulation of a conditionally-stable power cycle

Using the Matlab ode45 function to solve Equation (1), and by adopting the following: the same mass and stiffness parameters as in Section 4, switched values of the generator coefficient c_g, an Otto cycle, and an instantaenous heat-release model, and specified positions for the scavenge ports and spark timing, a conditionally-stable displacement response cycle can be obtained. The relevant parameters for the simulation are shown in Table 1. The performance and efficiency results from the simulations are shown in Table 2. Figure 4 shows the simulated cylinder PV diagram for the cycle, i.e. the combustion pressure versus the displaced volume for the generator in a conditionally-stable power cycle

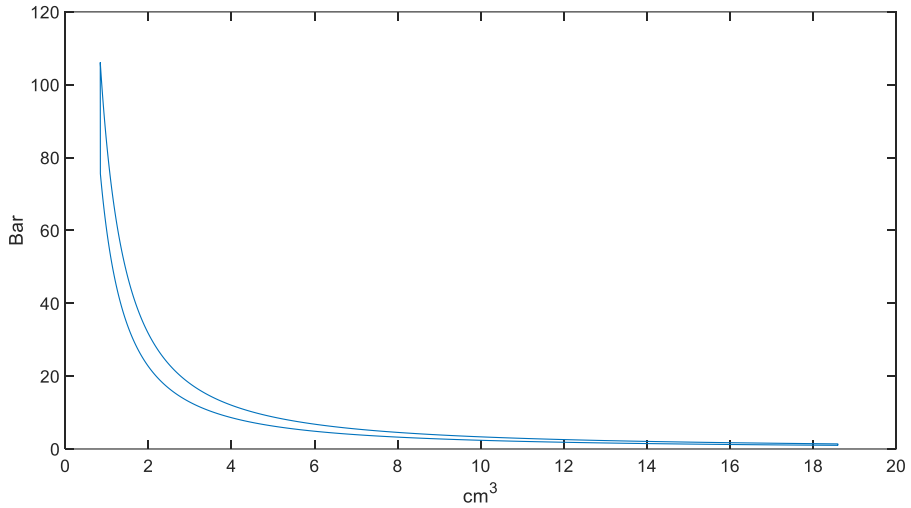

Figure 4: Simulated combustion pressure versus displaced volume (i.e. the PV diagram) for the generator in a conditionally-stable resonant Otto cycle.

Generator Parameters	Cylinder length = 28.16 mm. Bore = 29 mm.	Mass of moving assembly m = 0.42 kg.	Resilient member Spring stiffness *k* = 60000 N/m	Magnitude of generator coefficient during compression: Cg = 5.2; during expansion: Cg = 9.9
Key event positions	Distance of displacement *x* from equilibrium to scavenge ports = -12.8 mm.	Distance of displacement *x* from equilibrium to spark ignition event = 14.0812 mm.		
Simulation and model details	Number of discrete points per cycle = 80000.	Start displacement = -25.6 mm; End displacement = -25.6002 mm.	Difference between start and end displacement = -0.0002097 mm.	Linear damping factor (during compression) = 1.63% critical.

Table 1: Generator, simulation, and model parameters

Temperatures and pressures	Start of compression temperature: 300 K at pressure of 1 bar.	End of compression temperature: 1033.48 K at pressure of 75.88 bar.	After heat-release temperature: 1444.45 K at pressure 106.06 bar.	End of compression Temperature : 419.29 K at pressure of 1.40 bar.	After scavenging temperature: 300 K at Pressure of 1 bar
Power	Target power = 500 W	Average mechanical power = 357.1367 W	Average electrical generator power = 357.1126 W.	Peak instantaneous mechanical power = 16856 W	Peak instantaneous electrical power = 892 W
Efficiencies	Otto efficiency = 70.9747%	Indicated thermal efficiency using (Qin+Qrej)/Qin = 70.9723%.	Indicated thermal efficiency using WD/Qin = 71.4511%.	Generator efficiency (electrical power out/target power) = 71.4225%.	Assumed electrical machine efficiency = 100%
Phase information	Phase of the fundamental harmonic component of excitation force = -96.16°	Phase of the fundamental harmonic component of displacement response = -91.29°	Phase difference between the fundamental harmonic components of the output and input = +4.86°	Notation: Positive phase is advance; Negative phase is delay.	

Table 2: Simulation results

For the parameters used in Equation (1) as given in Table 1, Figure 5 shows the simulated conditionally-stable force-displacement trajectories for the combustion side of the generator (left), and correspondingly, for electrical machine side (right). The area under left-hand Figure 5 gives the (indicated) mechanical energy released within the cycle, whereas the area under right-hand Figure 5 gives the electrical energy generated within the cycle (assuming 100% efficient electrical energy conversion). Figure 6 shows, over one conditionally-stable cycle, the simulated instantaneous and average mechanical power versus time. Figure 7 shows the corresponding instantaneous and average electrical power versus time.

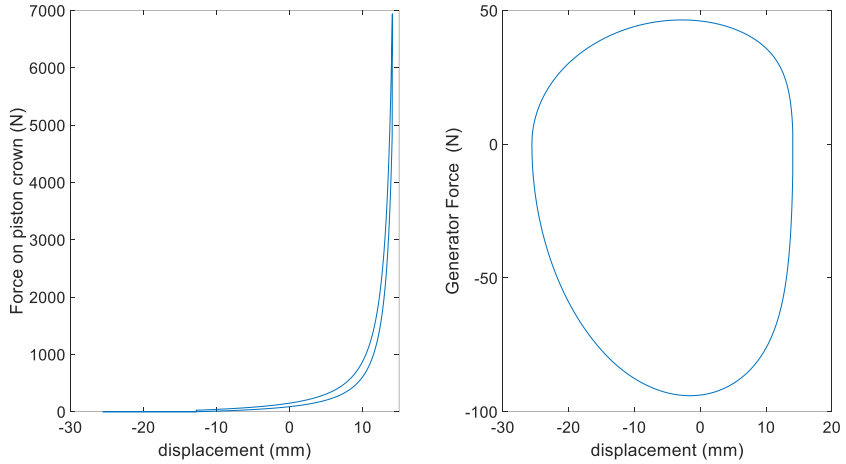

Figure 5: Force-displacement trajectories: for the combustion side of the generator (left), and corresponding for the electrical machine (right).

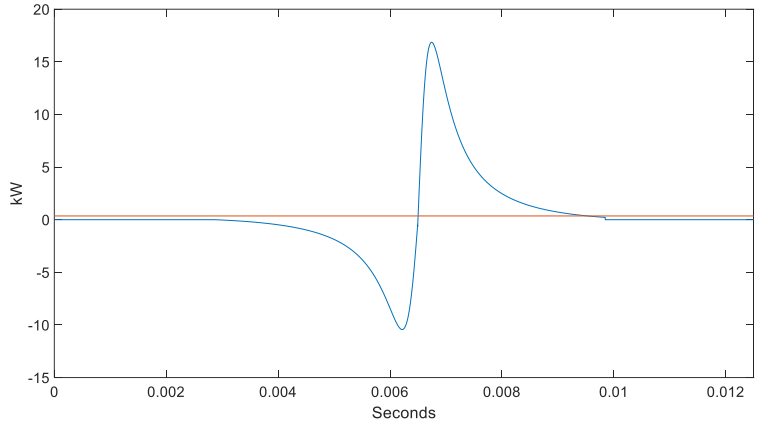

Figure 6: Instantaneous and average mechanical power versus time over a cycle.

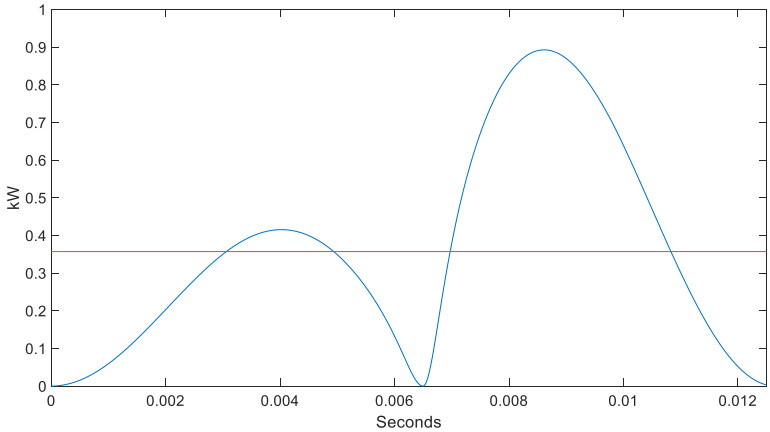

Figure 7: Instantaneous and average electrical power versus time over a cycle.

Figure 8 shows, for a complete cycle, the force on the piston crown as a function of time, synchronised with the corresponding displacement response. The maximum value of the displacement response is located by the dashed line (in red). To compute the phase difference between the gas pressure excitation force and the displacement response, and to establish how much the excitation and response deviate from being pure sine waves, Fourier analysis has been undertaken. The phase difference of +4.86° (given in Table 2) was calculated in terms of the difference between the fundamental components of the excitation and response. Figure 9 shows the first 20 harmonic components (cosine and sine components) of the force associated with the gas pressure excitation. The bottom Figure 9 shows the corresponding magnitudes of force harmonics.

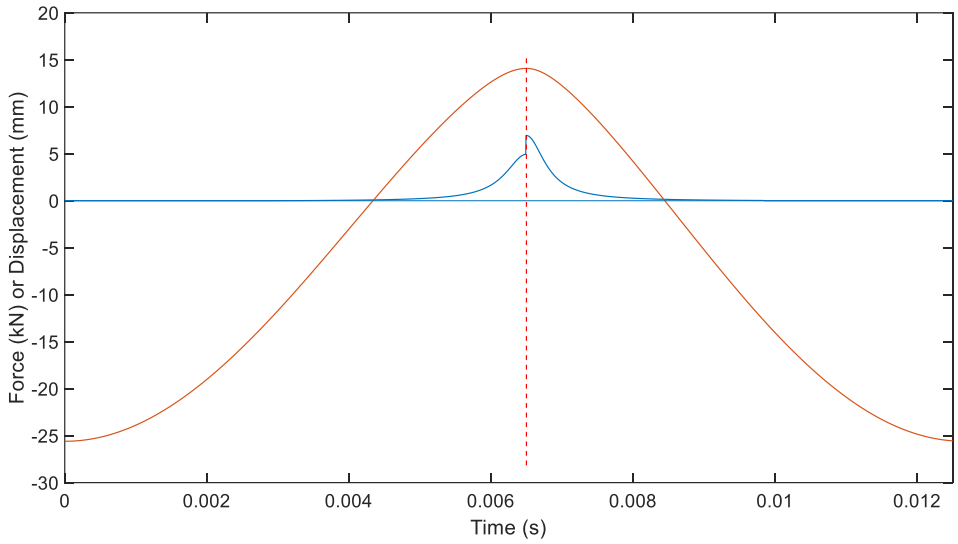

Figure 8: An excitation (force trace) and displacement response cycle; the dashed line locates the maximum of the displacement response.

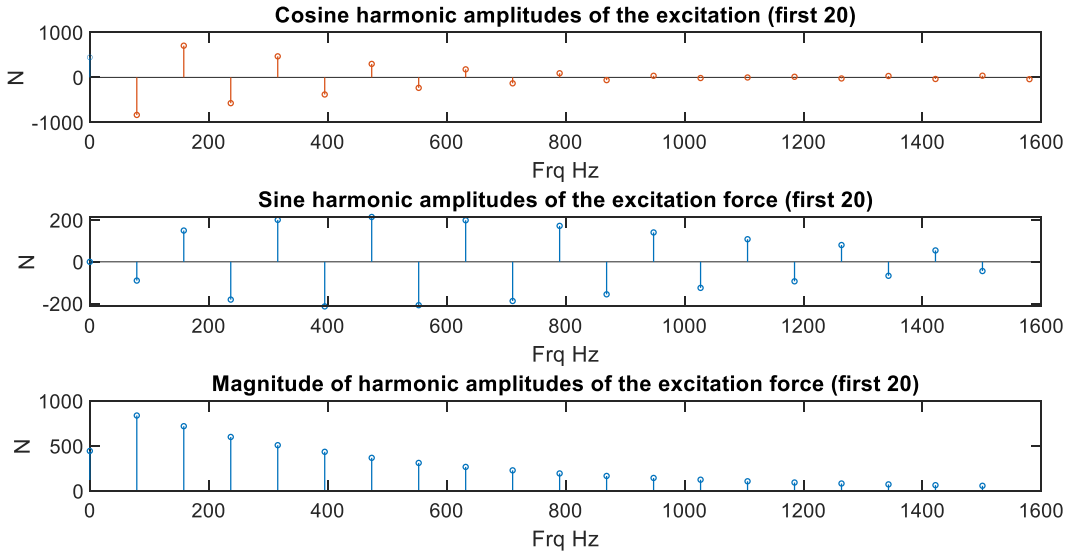

Figure 9: Fourier coefficients for the combustion-gas pressure induced excitation force: cosine terms (top); sine terms (middle); magnitudes (bottom).

Figure 10 shows the first 20 harmonic components (cosine and sine components) for the displacement response. The bottom Figure 10 shows the corresponding magnitudes of the displacement harmonics.

5.2 Discussion of Results

The resonant starting results shown in Figures 2 and 3, confirm that the phase difference using steady-state resonance is very different from linear theory. The results show that the nonlinear effects of adiabatic compression and expansion, although of weak stiffness compared with the resilient linear spring stiffness, significantly affects the phase, when excited at the (nonlinear) resonant frequency of 78.994 Hz. The

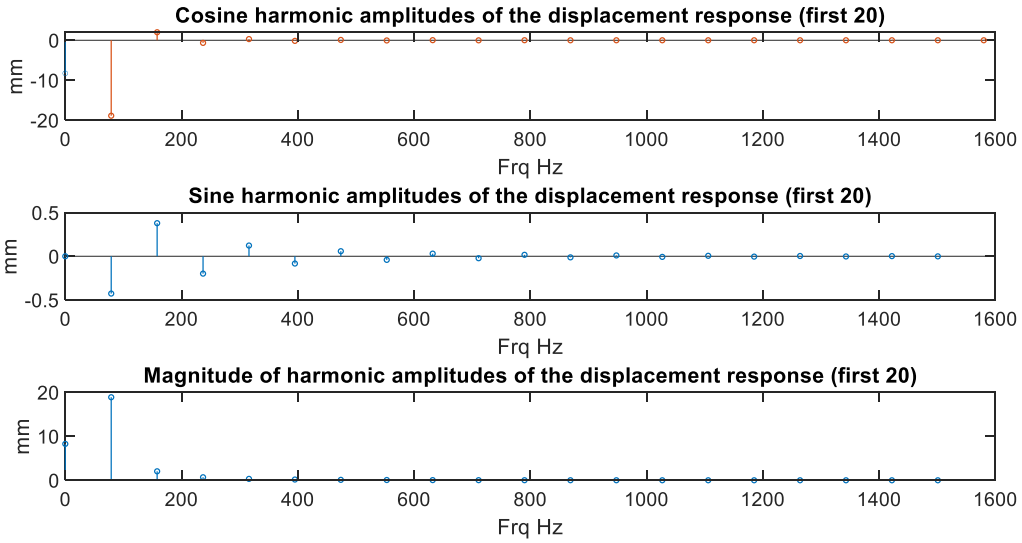

Figure 10: Fourier coefficients for the generator displacement response: cosine terms (top); sine terms (middle); magnitudes (bottom).

phase difference between the response fundamental harmonic and the excitation is -15.25°. The effect on the phase difference, of adiabatic compression, expansion, and then scavenging (collectively, an augmented form of asymmetric nonlinearity), is therefore quite stark, in the sense that it produces a reduction in the delay by 74°. Although not discussed in any detail, the system proves extremely sensitive to changes in both excitation and frequency. It is evident that the magnitude of the negative overshoot in the bottom Figure 2, would be highly undesirable. Fortunately, alternative resonant starting methods are available [14] which when implemented, would not generally require having to wait until a steady-state response displacement has been reached (which would take too long and would probably use too much energy). Rather, an optimal excitation can be obtained to excite the system in order to rapidly reach the starting amplitude. Nonlinear optimal exciter solution methods are available although the computaional demand is not insignificant. Nonetheless, the phase difference information obtained here will still be relevant for all the other starting methods.

Regarding the self-excited resonant response, the numerical simulation result of +4.86° for the phase difference between self-excitation and the response for a conditionally-stable power cycle, provides an answer to the importance of phase. It is evident that the phase difference of the fundamental harmonic of the self-excitation and the fundamental harmonic component of the displacement response represents a small phase advance of +4.86°. The implications of this finding for making the transition from resonant starting to self-excited operation (involving fired combustion) is that when the required displacement amplitude is predicted to be reached, fuel injection needs to have started at the beginning of that particular cycle. Consequently, the resonant starting excitation must end, and a spark event must appropriately occur, before the advance phase angle of the displacement is reached.

6 Conclusions

The phase differences between the excitation force and the response of a resonating free piston engine generator, have been examined by numerical simulation, for both resonant starting, and self-excited resonant combustion. The resonant starting results show that the system is highy sensitive to small changes in amplitude and frequency. The results also show for resonant starting, that for harmonic excitation at the (nonlinear) resonant frequency, the response is moderately delayed, almost in phase with the excitation Under resonant operating conditions, the phase difference between the fundamental harmonic of the self-excitation and the fundamental harmonic component of the displacement response is very small, suggesting the excitation and response are almost in phase. The implications of this finding for making the transition from resonant starting to self-excited operation (involving fired combustion), is that when the required displacement amplitude is predicted to be reached, fuel injection needs to have already occurred, and appropriate spark timing chosen.

References

[1] A. Smallbone, M. R. Hanipah, B. Jia, T. Scott, J. Heslop, B. Towell, C. Lawrence, S. Roy, K. V. Shivaprasad, and A. P. Roskilly (2020) *Realization of a Novel Free-Piston Engine Generator for Hybrid-Electric Energy & Fuels*, 2020 *34* (10), 12926-12939 DOI: 10.1021/acs.energyfuels.0c01647

[2] C. Depcik, T. Cassady, B. Collicott, S.P. Burugupally, X. Li, S. Saud Alam, J. Rocha Arandia, J. Hobeck (2020) Compar*ison of lithium ion Batteries, hydrogen fueled combustion Engines, and a hydrogen fuel cell in powering a small Unmanned Aerial Vehicle*, Energy Conversion and Management Volume 207, 1 March 2020, 112514 https://doi.org/10.1016/j.enconman.2020.112514.

[3] Y. Woo, Y. Lee and Y. Lee. (2009) *The performance characteristics of a hydrogen-fuelled free piston internal combustion engine and linear generator system*, International Journal of Low-Carbon Technologies 2009, 4, 36–41. doi:10.1093/ijlct/ctp003

[4] C. Yuan, Y. Jing, C. Liu, Y. He. (2019) *Effect of variable stroke on fuel combustion and heat release of a free piston linear hydrogen engine.* International Journal of Hydrogen Energy. Volume 44, Issue 36, 26 July 2019, Pages 20416-20425. https://doi.org/10.1016/j.ijhydene.2019.05.232

[5] C. Yuan, H. Ren, Y. Jing, J. Xu, Y. He (2019) *The effect of motion on fuel diffusion and mixture preparation of a free-piston linear hydrogen engine*, International Journal of Hydrogen Energy Volume 44, Issue 10, 22 February 2019, Pages 4996-5006. https://doi.org/10.1016/j.ijhydene.2018.12.197

[6] C. Yuan, Y. Jing, Y. He, S. Zeng. (2020) *Multidimensional analysis of the impact of motion variation on exergetic performance in a free piston linear hydrogen engine*, International Journal of Hydrogen Energy Volume 45, Issue 51, 16 October 2020, Pages 27864-27875. https://doi.org/10.1016/j.ijhydene.2020.07.072

[7] Z. Zhang, H. Feng and Z. Zuo (2020) *Numerical Investigation of a Free-Piston Hydrogen-Gasoline Engine Linear Generator*, Energies 2020, 13, 4685; doi:10.3390/en13184685

[8] E**.** Z. Zainal A**.,** S**.** E. Mohammed, A.R**.**A. Aziz, M. B. Baharom, **and** A Jaffry, Firmansyah, A. Shahrul A**.**, M**.** A. Ismael (2021) *Effect of aspect ratio on the performance characteristics of free piston linear*

[9] U. Ngwaka, D. Wu, J. H. Smith, B. Jia, A. Smallbone, C. Diyoke, and A. P. Roskilly. (2021) *Parametric analysis of a semi-closed-loop linear joule engine generator using argon and oxy-hydrogen combustion*, Energy. Volume 217, 15 February 2021, 119357. https://doi.org/10.1016/j.energy.2020.119357

[10] D. Liu, C. Yuan. (2022) *A coupling study of ignition position on fuel-air mixing and diffusion of a linear hydrogen engine*, International Journal of Hydrogen Energy. Volume 47, Issue 89, 1 November 2022, Pages 38018-38030. https://doi.org/10.1016/j.ijhydene.2022.08.274

[11] M. Pyrc, M. Gruca, W. Tutak, and A. Jamrozik. (2023) *Assessment of the co-combustion process of ammonia with hydrogen in a research VCR piston engine.* International Journal of Hydrogen Energy Volume 48, Issue 7, 22 January 2023, Pages 2821-2834. https://doi.org/10.1016/j.ijhydene.2022.10.152

[12] J. F. Dunne (2010) *Dynamic Modelling and Control of Semi-Free-Piston Motion in a Rotary Diesel Generator Concept*, ASME Journal of Dynamic Systems, Measurement, and Control, Vol 132 (5), (September 2010).

[13] T. N. Kigezi, and J. F. Dunne (2017) *A model-based control design approach for linear free-piston engines*, Journal of Dynamic Systems, Measurement and Control. 139 (11). ISSN 0022-0434.
generator engine fueled by hydrogen, International Journal of Hydrogen Energy Volume 46, Issue 17, 8 March 2021, Pages 10506-10517. https://doi.org/10.1016/j.ijhydene.2020.12.122

[14] T. Kigezi, J. F. Dunne (2017) *Optimal starting control for a nonlinear resonating free piston generator*, 14th International Conference Dynamical Systems - Theory and Applications December 11-14, 2017. Lodz, Poland. 12 pages.

[15] S. A. Zulkifli, M. N. Karsiti and A. R. A. Aziz (2008) *Starting of a free-piston linear engine-generator by mechanical resonance and rectangular current commutation*, IEEE Vehicle Power and Propulsion Conference (VPPC), September 3-5, 2008, Harbin, China.